TITLE

Theoretical investigation of superconductivity in the non-centrosymmetric SrPtGe3 and CaPtSi3 compounds

AUTHORS

Uzunok, HY; Tütüncü, HM; Srivastava, GP; et al.

JOURNAL

DEPOSITED IN ORE

07 January 2019

Ab initio investigation of electron-phonon interaction in LaSn$_3$ and CaSn$_3$

H. Y. Uzunok[1,2], H. M. Tütüncü[*1,2], Ertuğrul Karaca[2], A. Başoğlu[1], G. P. Srivastava[3]

[1]Sakarya Üniversitesi, Fen-Edebiyat Fakültesi, Fizik Bölümü, 54187, Adapazarı, Turkey

[2]Sakarya Üniversitesi, Biyomedikal, Manyetik ve Yarıiletken Malzemeler Araştırma Merkezi (BIMAYAM), 54187, Adapaz arı, Turkey

[3]School of Physics, University of Exeter, Stocker Road, Exeter EX4 4QL, UK

We present results for the structural, electronic, vibrational, and electron-phonon coupling properties of LaSn$_3$ and CaSn$_3$ adopting the simple cubic AuCu$_3$-type structure obtained using the the generalized gradient approximation of the density functional theory and plane wave *ab initio* pseudopotential method. Our electronic results show that both materials display metallic character with several bands, which have mainly Sn 5p character, crossing the Fermi level. The calculated phonon spectrum of LaSn$_3$ accords very well with reported experimental measurements. The weights of the peaks in the Eliashberg spectral function of both compounds are enhanced with the use of experimental lattice constant in our electron-phonon calculation, increasing the value of average electron phonon coupling parameter from 0.876 to 0.937 for LaSn$_3$ (by 7%) and from 0.642 to 0.725 for CaSn$_3$ (by 13%). The use of experimental lattice constant also improves the agreement between theoretical and experimental values of the superconducting temperature for both compounds.

1 Introduction

The RX$_3$ (R = rare earth elements, X = In, Sn, Tl, Pb) intermetallic materials adopting the simple cubic AuCu$_3$-type structure have received a large deal of attention from the scientific community because of their various properties changing from magnetism to superconductivity [1–30]. Some of these compounds, such as PrSn$_3$ and NdSn$_3$ exhibit antiferromagnetic ordering with the Néel temperatures of 8.6 and 4.5 K [2, 10]. In addition, PrSn$_3$ and CePb$_3$ are also known as heavy-fermion compounds [15, 23], while CeSn$_3$ has been classified as a dense Kondo compound displaying valence fluctuations [15, 20]. Furthermore, the LaX$_3$ (X = In, Sn, Tl, Pb) compounds have received considerably more attention than other AuCu$_3$-type compounds because they all display superconductivity. The superconducting transition temperature of LaSn$_3$ is reported to be around 6.5 K [1, 6, 27], which is relatively larger than the corresponding value for LaIn$_3$, LaPb$_3$ and LaTl$_3$ [3, 7, 27, 30]. The average electron-phonon coupling parameter of LaSn$_3$ has been reported to be 0.80 in the experimental work of Toxen and co-workers [5], which suggests that the electron-phonon interaction in this superconductor is of medium strength.

The existence of superconductivity in LaSn$_3$ motivated several theoretical groups [31–35] to investigate its structural, elastic and electronic properties. Koelling [31] has been performed self-consistent linearized augmented plane wave (LAPW) calculations for the Fermi surface topology of LaSn$_3$. The linearized muffin-tin-orbital method with the atomic sphere approximation (LMTO-ASA) [32] has been utilized to determine the electronic band structure of LaSn$_3$. This theoretical [32] work suggests that LaSn$_3$ acts like a transition metal compound since the bonding state in this material is due to the interaction between La d and Sn p states. The electronic structure, Fermi surface, and elastic properties of LaSn$_3$ have been reported in the full-potential linear augmented wave (FP-LAPW) work of Ram and co-workers [33], utilizing both the local density approximation (LDA) and generalized gradient approximation. This work finds that the second order elastic constants of LaSn$_3$ increase with pressure and meet the mechanical stability conditions under pressure. Abraham and co-workers [34, 35] have also used the FP-LAPW method to

---

* Corresponding author. Email: tutuncu@sakarya.edu.tr

investigate the structural, electronic, elastic and thermal properties of this superconductor. However, only the GGA method for the exchange correlation potential has been used in these theoretical works [34, 35]. These theoretical calculations [34, 35] confirm the metallic character and mechanical stability of LaSn$_3$.

Recently, magnetic susceptibility, electrical resistivity, and specific-heat measurements reveal that CaSn$_3$ exhibits superconductivity with a superconducting transition temperature of 4.2 K [36]. The magnetization versus magnetic field (M-H) curve displays the typical type-II behavior [36]. In this work [36], the electronic band structure and electronic total density of states for this superconductor have been presented by using the density functional theory. This study [36] reveals that the electronic states around the Fermi level for CaSn$_3$ have been dominated by the p states of Sn atoms.

Although the electronic properties of LaSn$_3$ and CaSn$_3$ have been reported and discussed in the literature, in order to get a deeper insight into their superconducting properties, the electron-phonon interaction study for them is certainly needed. This, in turn, requires a detailed study of the vibrational properties of these compounds, since phonons essentially are responsible for the coupling between electrons to form Cooper pairs required in the BCS theory. Inelastic neutron scattering techniques [11] have been utilized to measure the phonon dispersion curves of LaSn3 at room temperature. This experimental work [11] signals the dynamical stability of LaSn$_3$ in its AuCu$_3$-type structure. Recently, the electron spin resonance study [27] of the LaIn$_{3-x}$Sn$_x$ superconducting system reveals that the superconducting T_c displays an oscillatory dependence as a function of Sn substitution, taking its smallest value of around 0.70 K for LaIn$_3$ and the largest value of $\approx$ 6.4 K for the LaSn$_3$ end member.

In this work we aim to gain a detailed understanding of the origin of superconductivity in these superconductors by studying their electron-phonon interaction properties. With this in mind, we report and discuss our results on the structural, electronic, phonon and electron-phonon interaction properties of LaSn$_3$ and CaSn$_3$ using *ab initio* pseudopotential method based on a generalized gradient approximation of density functional theory. After comparing our results with those presented in previous theoretical results [31–35], we extend our calculations with the application of a linear response scheme [37] to investigate the lattice dynamical properties of both compounds using their theoretical and experimental lattice parameters. Our phonon dispersion curves for LaSn$_3$ are compared with the inelastic neutron scattering results [11]. After obtaining phonon properties of LaSn$_3$ and CaSn$_3$, the Eliashberg spectral function for both superconductors is obtained from their calculated phonon density of states and their calculated electron-phonon matrix elements. Finally, the superconducting temperature estimated from the Allen-Dynes modified McMillan equation [38] has been compared with experimentally deduced results [6, 36].

2 Theory

All our calculations have been carried out using the density functional theory (DFT) implemented in Quantum-Espresso code [37]. The exchange and correlation effects are included within the generalized gradient approximation (GGA), utilizing the revised scheme of Perdew-Burke-Ernzerhof (PBE-sol) [39]. The energy convergence is checked with respect to the energy cutoff and $\boldsymbol{k}$-point sampling. We utilize ultrasoft pseudopotentials [40, 41] and the planewave basis set with the energy cutoff of 60 Ry and 600 Ry for wave function and charge density, respectively. Self-consistent solutions of the Kohn-Sham equations [42] are obtained by employing a set of Monkhorst-Pack special $\boldsymbol{k}$ points [43] within the irreducible part of the Brillouin zone (IBZ). The Brillouin zone integration for total energy calculations has been carried out using a (12×12×12) $\boldsymbol{k}$ mesh while a denser (48×48×48) $\boldsymbol{k}$ mesh is used to obtain the electronic properties of the studied compounds. We believe that the 48×48×48 $\boldsymbol{k}$ mesh is more than enough for electronic and electron-phonon interaction calculations in LaSn$_3$ and CaSn$_3$, as previous stuies by Dugdale [44] have studied electronic and electron-phonon interactions properties of YSn$_3$ by only using 32×32×32$\boldsymbol{k}$ mesh.

The phonon calculations have been performed by using the density functional perturbation theory in the linear response approach [37]. The Brillouin zone integration for phonon calculations has been implemented using a (12×12×12) $\boldsymbol{k}$ mesh. As phonon calculations are computationally very demanding, we first calculated dynamical matrices on the (6×6×6) Monkhorst-Pack grid which corresponds to 20 speical $\boldsymbol{q}$ points. Then, they are Fourier transformed to investigate phonon modes for any chosen $\boldsymbol{q}$ point. The DFT also supplies a confident first-principles framework for implementing the Migdal-Eliashberg approach

for obtaining superconducting properties of crystals. The essential part of this approach is the Eliashberg spectral function ($\alpha^2F(\omega)$) [37, 38, 45–47] which can be given in terms of the phonon linewidth $\gamma_{\boldsymbol{q}j}$ of mode j at wavevector $\boldsymbol{q}$ by

$$\alpha^2F(\omega) = \frac{1}{2\pi N(E_F)} \sum_{\mathbf{q}j} \frac{\gamma_{\mathbf{q}j}}{\hbar\omega_{\mathbf{q}j}} \delta\left(\omega - \omega_{\mathbf{q}j}\right), \tag{1}$$

where $\omega_{\boldsymbol{q}j}$ is the phonon frequency and $N(E_F)$ presents the electronic density of states per atom and spin at the Fermi level. $\gamma_{\boldsymbol{q}j}$ stemming from electron-phonon interaction [37, 38, 45–47] can be expressed as

$$\gamma_{\mathbf{q}j} = 2\pi\omega_{\mathbf{q}j} \sum_{\mathbf{k}nm} |g^{\mathbf{q}j}_{(\mathbf{k}+\mathbf{q})m;\mathbf{k}n}|^2 \delta(\varepsilon_{\mathbf{k}n} - \varepsilon_F)\delta(\varepsilon_{(\mathbf{k}+\mathbf{q})m} - \varepsilon_F), \tag{2}$$

where $\varepsilon_{(\mathbf{k}+\mathbf{q})m}$ and $g^{\mathbf{q}j}_{(\mathbf{k}+\mathbf{q})m;\mathbf{k}n}$ are the energies of bands and the electron-phonon matrix element, respectively. The electron-phonon interaction matrix is calculated by self-consistent calculations via the following formula; [37, 48]

$$g^{\mathbf{q}j}_{(\mathbf{k}+\mathbf{q}),m;\mathbf{k}n} = \sqrt{\frac{\hbar}{2M\omega_{\mathbf{q}j}}} \left\langle \phi_{(\mathbf{k}+\mathbf{q})m}|\mathbf{e}_{\mathbf{q}j} \cdot \vec{\nabla}V^{SCF}(\mathbf{q})|\phi_{\mathbf{k}n} \right\rangle. \tag{3}$$

Here M is a convenient reference mass and $\vec{\nabla}V^{SCF}(\mathbf{q})$ is the derivative of the self-consistent effective potential with respect to a collective ionic displacement corresponding to a phonon with branch index j and momentum $\mathbf{q}$. The self-consistency calculations include some approximated electronic screening schemes, which are simply called Thomas-Fermi, and local Thomas-Fermi mixing [49]. It is worth to mention that Fröhlich interaction is also considered during the calculation of electron-phonon matrices [48, 50].

The contribution of each vibrational mode to the electron-phonon coupling parameter can be obtained from the following equation:

$$\lambda_{\mathbf{q}j} = \frac{\gamma_{\mathbf{q}j}}{\pi\hbar N(\varepsilon_F)\omega^2_{\mathbf{q}j}}. \tag{4}$$

The average electron-phonon coupling parameter λ can be determined from the summation of $\lambda_{\boldsymbol{q}j}$ over all phonon modes ($\boldsymbol{q}$j) in the IBZ,

$$\lambda = \sum_{\boldsymbol{q}j} \lambda_{\boldsymbol{q}j}W(\boldsymbol{q}). \tag{5}$$

Here W($\boldsymbol{q}$) is the weight of a sampling $\boldsymbol{q}$ point in the IBZ. The value of logarithmically averaged frequency $\omega_{\ln}$ can be given by the following equation [37, 38, 45, 46]:

$$\omega_{\ln} = \exp\left(\frac{1}{\lambda}\sum_{\boldsymbol{q}j} \lambda_{\boldsymbol{q}j}\ln\omega_{\boldsymbol{q}j}\right). \tag{6}$$

Then, T_c is evaluated from the Allen-Dynes modified McMillan equation [38] which is given as:

$$T_c = \frac{\omega_{\ln}}{1.2}\exp\left(-\frac{1.04(1+\lambda)}{\lambda - \mu^*(1+0.62\lambda)}\right). \tag{7}$$

Here, where μ^* is a Coulomb pseudopotential and its value usually changes between 0.10 and 0.16 [38]. Following a recent experimental work [36], the value of μ^* is set to 0.10 in this theoretical work. Finally,

we have to specify that a denser ($36{\times}36{\times}36$) $\boldsymbol{k}$ mesh is used for the electron-phonon coupling calculations, which need more attentive treatment of the Fermi energy E_F .

3   Results

3.1   *Structural and Electronic Properties*

LaSn$_3$ and CaSn$_3$ both belong to the simple cubic AuCu$_3$-type structure (Pm$\overline{3}$m space group), where the number of atoms in the unit cell corresponds to the formula unit. The positions of four atoms are enforced by symmetry: La (or Ca) fills the (1a) site $(0, 0, 0)$ and three Sn (3c) sites at $(1/2, 1/2, 0)$. As a consequence, La (or Ca) atoms occupy the simple cubic lattice points, while Sn atoms are octhahedrally coordinated to each other, as illustrated in Fig. 1(a). Each Sn atom is in four-fold coordination constituted by four La (or Ca) atoms, while each La (or Ca) atom is surrounded by twelve Sn atoms, as shown in Fig. 1(b). The value of nearest neighbour distance (d) is calculated to be 3.351 $\AA$ for LaSn$_3$ and 3.319 $\AA$ for CaSn$_3$. These values are even smaller than the sum of the atomic radii of La (or Ca) and Sn (which is around 3.40 $\AA$). This result signals strong bonding between La (or Ca) and Sn atoms. The equilibrium lattice constant (a), the bulk modulus (B), and its first order pressure derivative ($B^{'}$) are determined by minimizing the crystal total energy for different values of the lattice constant by means of Murnaghan equation of state [51]. The calculated values of a, equilibrium volume (V), d, B and $B^{'}$ are presented in Tab. 1 along with existing experimental [3, 11, 36] and theoretical results [32–35]. In general, our results are in acceptable accordance with available experimental [3, 11, 36] and theoretical results [32–35]. In particular, the calculated lattice constants of LaSn$_3$ and CaSn$_3$ differ from their experimental values [3, 36] of 4.771 $\AA$ and 4.742 $\AA$ by 0.7% and 1.0%.

The electronic structure and electronic density of states (DOS) for LaSn$_3$ are depicted in Fig. 2. In general, the whole band structure outline is similar to previous theoretical results [33–35]. In particular, the calculated electronic band structure signals the metallic property since at least one energy band crosses the Fermi level along the principal symmetry directions. In order to define specific electronic states connected with the superconducting properties due to electron-phonon interaction, the total and partial DOS must be examined in detail. The valence band region extending from -10.6 eV to the Fermi level can be divided into two parts which are separated from each other by a pseudo gap at around -4.6 eV. The lower part is mixed of Sn 5s, La 6p, Sn 5p and La 5d states with the main contribution from the first one. The higher part consists mainly of the p electrons of Sn which hybridizes with the d states of La. This hybridization is the source of bonding between La and Sn atoms. As electrons near the Fermi level have the potential to constitute Cooper pairs, it is compulsory to examine their nature in more detail. First, the Fermi level lies at the flank of a local maximum of DOS, proposing that this compound is a good candidate to display superconductivity. Secondly, the metallic behavior of LaSn$_3$ is also confirmed by the existence of finite DOS at the Fermi level. Thirdly, the DOS in the vicinity of the Fermi level is mainly dominated by the p states of Sn atoms with considerable contribution from the d states of La atoms. Finally, the total DOS at the Fermi level ($N(E_F)$) amounts to be 2.582 States/eV which is in good accordance with its experimentally reported value [5] of 2.60 States/eV. When the spin-orbit coupling(SOC) is considered, this value is changed from 2.582 States/eV to 2.607 States/eV, the difference being less then 1.0%. This reveals that the effect of SOC on the electronic bands close to Fermi level is negligible. Since Cooper pairs in the BCS theory are constituted by electrons having energies close to the Fermi level, we did not consider the SOC in our calculations. We have to mention that similar observation has been made for YSn$_3$ in the theoretical work of Dugdale [44]. A critical assessment of the partial DOS reveals that the value of $N(E_F)$ is contributed approximately by 69% from Sn electronic states and 31% from La electronic states. In particular, 60% of $N(E_F)$ comes from only Sn 5p states. This result suggests that Sn 5p electrons have a great potential to form Cooper pairs and thus influence the superconducting state of LaSn$_3$.

Fig. 3 presents the calculated energy band structure and density of states (DOS) for CaSn$_3$. This compound also exhibits metallic character with valence and conduction like bands of mainly Sn 5p character, crossing the Fermi level, compatible with the results of Luo and co-workers [36]. In general, the contribution of Ca atoms to valence band region is much smaller than that of Sn atoms but the partial DOS of

Ca are considerably present above the Fermi level. This result reveals that the bonding mechanism of this superconductor can be considered as a charge transfer from Ca to Sn. In particular, the low energy region of valence band, below -4.4 eV, is primarily formed by Sn 5s states but that a measurable contribution from Sn 5p, Ca 3d and Ca 4s states also exists. The main valence band region of this superconductor extends from -4.4 eV to the Fermi level. This region is almost dominated by the p states of Sn atom which hybridize with Ca 3d and Sn 5s states. Different from LaSn₃, the Fermi level almost lies at the dip of a local minimum of DOS, resulting in a small $N(E_F)$ value of 1.215 States/eV. It is worth to mention that this value nearly does not change by the inclusion of SOC. This small value is one of the reasons why the T_c value of CaSn₃ is smaller than that of LaSn₃ since the smaller value of $N(E_F)$ decreases the value of the electron-phonon coupling parameter according to the McMillan expression ($\lambda = \frac{N(E_F)<I^2>}{M<\omega^2>}$), where $<I^2>$, $<\omega^2>$ and M are the averaged square of the electron-phonon matrix element, the averaged square of the phonon frequency, and the mass involved, respectively. A critical examination of the DOS indicates that that mainly Ca (% 21), and Sn (% 79) electronic states contribute to $N(E_F)$. This observation suggests that the origin of superconductivity in CaSn₃ stems from the p states of Sn atoms while the effect of Ca electronic states is negligible.

3.2 *Electron-Phonon interaction*

A confident investigation of electron-phonon interaction certainly requires the knowledge of the full phonon spectrum throughout the BZ. The calculated phonon dispersion relations for LaSn₃ are illustrated in Fig. 4(a). The solid lines and dashed lines display the phonon branches calculated with the use of theoretical and experimental values of lattice parameter, respectively. Filled red squares are inelastic neutron scattering results [11]. In general, our both results are in good agreement with inelastic neutron scattering results [11]. This agreement reveals the good accuracy of our phonon calculations. Although, the calculated value of lattice parameter for LaSn₃ slightly differs from its experimental value (see Tab. 1), the use of experimental lattice parameter makes a significant difference for the phonon property of this superconductor. We find that the consideration of the experimental lattice constant (which is 0.7% higher for LaSn₃ and 1% higher for CaSn₃) almost decreases the frequency of all phonon branches and thus increases the electron-phonon coupling parameter according to Eq. 4, which in turn causes an increase in the value of T_c.

Most of phonon branches for LaSn₃ exhibit considerable amount of dispersion, leaving no gap in the phonon spectrum. The total and partial phonon density of states are presented in Fig. 4 (b). The total DOS also confirms the softening of phonon branches with the use of experimental lattice constant. The width of total DOS decreases from 4.5 THz to 4.3 THz when the experimental lattice constant is used for our phonon calculations. The partial DOS of reveals that the contribution of Sn-related phonon densities is dominant over the whole range of phonon frequencies. In particular, in the frequency ranges 1.6-2.7 THz and 3.5-4.5 THz, a substantial La-Sn hybridization is present. However, a much smaller La contribution exist in the frequency ranges 0.0-1.6 THz and 2.7-3.5 THz. From the examination of partial phonon DOS and partial electronic DOS, we can conclude that while the Sn-related vibrations are present in the entire frequency range, the partial electronic DOS of Sn states are considerably present below the Fermi level. This observation suggests that Sn p states and Sn-related lattice vibrations have a strong potential to constitute the superconducting state of LaSn₃.

The calculated phonon curves and phonon density of states for CaSn₃ are presented in Fig. 5 (a) and Fig. 5 (b), respectively. Once again, the use of experimental lattice parameter in our phonon calculations makes all phonon branches of CaSn₃ softer. Different from LaSn₃, the phonon spectrum of CaSn₃ exhibits a phononic character with a forbidden gap of 1.3 THz which decreases to 1.2 THz with the use of experimental lattice parameter. This forbidden gap separates the phonon spectrum into two apparent regions: a low frequency region (LFR) (0-3.2 THz) and a high frequency region (HFR) (4.5-5.6 THz). The three acoustic and six optical phonon branches are present in the LFR while three optical phonon branches form the HFR. All phonon branches exhibit a considerable amount of dispersion. Examining the partial phonon DOS for CaSn₃, one can find that, as expected, Sn as the heavier atom in this material dominates the LFR of phonon DOS. A much smaller Ca contribution exists in this region. Thus, phonon branches in the LFR are expected to couple strongly with the electrons at the Fermi level due to the considerable

existence of Sn p electrons at the Fermi level. Above the phononic band gap, the contribution of Ca atom to the phonon branches is dominant because Ca has a much lighter mass than that of Sn atom. As a consequence, the motion of Ca atom is expected to play a relatively insignificant role in the formation of superconducting state for $CaSn_3$.

To recognize the strengths with which the different modes of atomic vibration couple to electrons, and hence can effect the superconducting properties significantly, we have shown the Eliasberg spectral function $(\alpha^2F(\omega))$ and the variation of the average electron-phonon coupling parameter with rising phonon frequency for both materials in Fig. 6. The corresponding results with the use of experimental lattice constants are also presented by dashed lines in this figure. As can be seen from this figure, electron-phonon interaction in $LaSn_3$ is stronger than in $CaSn_3$. This provides a second reason why the T_c value of $LaSn_3$ is larger than that of $CaSn_3$. A careful assessment of $\alpha^2F(\omega)$ indicates the importance of phonon modes between 1.2 and 3.5 THz for electron-phonon interaction in $LaSn_3$, since the value of λ rises rapidly with increasing phonon frequency in this frequency region. The additive of these phonon modes to λ is as much as 81%. This result is largely expected because atomic vibrations in this frequency region involve mainly Sn atoms and their p electrons dominate the electronic states around the Fermi energy. As a consequence, these phonon modes of $LaSn_3$ couple strongly with electrons at the Fermi level. The examination of $\alpha^2F(\omega)$ for $CaSn_3$ signals the importance of phonon modes below the phononic gap region for electron-phonon interaction. In this region, the value of λ increases almost linearly with rising phonon frequency. The additive of these phonon modes to λ is approximately 90%. As the mass of Sn atom is much heavier than that of Ca atom, Sn atom dominates the vibrational states below the gap region. However, dominance of Ca atom exists above the gap region. Thus, the phonon modes below the gap region are more strongly involved in the process of scattering of electrons than the phonon branches above this region. As a result, for both materials, Sn-related phonon scattering plays a considerable role in the transition from the normal state to the superconducting state. Thus, we can conclude that superconductivity in both compounds seems to appear in an almost untainted BCS state.

As can be seen from Fig. 6, the weights of the peaks in the Eliashberg spectral function of both compounds are enhanced with the use of experimental lattice constant in our electron-phonon calculation. Thus, the experimental lattice constant-used enhancement of their λ values in Fig. 6 can be associated with both a softening of their phonon dispersion curves and an increase in their electron-phonon coupling matrix elements. The calculated values of the physical quantities with the use of theoretical and experimental values of lattice parameter associated with superconductivity in both superconductors and their comparison with available experimental [1, 5, 6, 9, 27, 36] and theoretical [32–35] results are presented in Tab. 2. The calculated values of $N(E_F)$, λ and T_c compare very well with their experimental values [1, 5, 6, 9, 27, 36]. When the experimental lattice constant is considered in our electronic calculations, the value of $N(E_F)$ for both materials is slightly increased. However, the use of the experimental lattice constant decreases the value of ω_{ln} for both materials. Thus, when the experimental lattice constant is used in our electron-phonon interaction, the value of λ is increased by 7% (from 0.876 to 0.937) for $LaSn_3$ and by 13% (from 0.642 to 0.725) for $CaSn_3$. As a consequence, the use of experimental lattice constant improves the agreement between theoretical and experimental values of T_c for both compounds (see Tab. 2).

4   Summary

In this work, we have investigated electron-phonon interaction in $LaSn_3$ and $CaSn_3$ crystallizing the simple cubic $AuCu_3$-type structure using the the generalized gradient approximation of the density functional theory and plane wave *ab initio* pseudopotential method. Our structural results for both compounds are in acceptable agreement with existing experimental and theoretical results. Our electronic results reveal metallic nature, with a few electronic bands which mainly possess Sn 5p character, crossing the Fermi level.

The calculated phonon spectrum of $LaSn_3$ are in satisfactory accordance with previously reported inelastic neutron scattering data. For this material, most of the phonon branches display a large amount of dispersion, leaving no gap in the phonon spectrum due to similarity in the atomic weights of La and Sn. However, different from $LaSn_3$, due to a significant difference in the atomic weights of Ca and Sn,

the phonon spectrum of CaSn$_3$ possesses a phononic character with a forbidden gap of 1.3 THz. For both compounds, when their experimental lattice parameters are used in our phonon calculations, all phonon branches become softer. This softening increases the average electron-phonon coupling parameter for both compounds, which in turn leads to an increase of the superconducting transition temperature for them.

The Eliashberg spectral function for both superconductors is obtained from the calculated phonon density of states and the calculated electron-phonon matrix elements. A detailed analysis of this spectral function reveals that Sn-related electron-phonon scattering in both materials plays a significant role in the transition from the normal state to the superconducting state due to the considerable presence of Sn p electrons at the Fermi level. The calculated value of the average electron-phonon coupling parameter λ is 0.876 for LaSn$_3$ and 0.642 for CaSn$_3$, which increase respectively to 0.937 and 0.725 with the use of the experimental lattice parameter. These increases can be related to both softening of the phonon dispersion curves and increase in the electron-phonon coupling matrix elements. Using the Allen-Dynes modified McMillian equation with the screened Coulomb pseudopotential parameter $\mu^* = 0.10$, the value of the superconducting temperature is evaluated to be 6.30 K for LaSn$_3$ and 3.80 K for CaSn$_3$, which are in acceptable agreement with the measured values of 6.45 and 4.20 K, respectively. Finally, we can conclude that superconductivity in both these compounds seems to appear in an almost untainted BCS state.

ACKNOWLEDGMENTS

References

[1] R. J. Gambino, N. R. Stemple, and A. M. Toxen, *Superconductivity of lanthanum intermetallic compounds with the Cu$_3$Au structure*, J. Phys. Chem. Solids 29 (1968), pp. 295-302.

[2] G. K. Shenoy, B. D. Dunlap, G. M. Kalvius, A. M. Toxen, and R. J. Gambino,*Magnetic and Structural Properties of Some RareEarthSn$_3$ Compounds*, J. Appl. Phys. 41 (1970), pp. 1317-1318.

[3] E. E. Havinga, H. Damsma, and M.H. van Maaren, *Oscillatory dependence of superconductive critical temperature on number of valency electrons in Cu$_3$Au-type alloys*, J. Phys. Chem. Solids 31 (1970), pp. 2653-2662.

[4] L. B. Welsh, A. M. Toxen, and R. J. Gambino, *Magnetic Properties of La Sn$_3$, Phys. Rev. B 4 (1971)*, pp. 2921-2931.

[5] A. M. Toxen, R. J. Gambino, and L. B. Welsh, *Microscopic and Macroscopic Electronic Properties of the AuCu$_3$ -Type Alloys: The LaSn$_3$-LaIn$_3$ Pseudobinary Alloy System*, Phys. Rev. B 8 (1973), pp. 90-97.

[6] P. Lethuillier, *Crystal-field effects on the superconducting transition temperature of LaSn$_3$:Pr, LaPb$_3$:Pr, and LaTl$_3$:Pr*, Phys. Rev. B 12 (1975), pp. 4836-4838 .

[7] L. B. Welsh, C. L. Wiley, and F. Y. Fradin, *Gd and Ce impurities in the LaX$_3$ compounds (X = I n , S n , P b): A nuclear-magnetic-resonance study*, Phys. Rev. B 11 (1975), pp. 4156-4167.

[8] S. Huang, C. W. Chu, F. Y. Fradin, and L. B. Welsh, *Anomalous Tc-behavior of LaSn$_3$ under pressure*, Solid State Commun. 16 (1975), pp. 409-412.

[9] L. E. Delong, M. B. Maple, and M. Tovar, *Superconducting and normal state properties of dilute alloys of LaSn$_3$ containing Ce impurities*, Solid State Commun. 26 (1978), pp. 469-475.

[10] J. M. Hastings, L. M. Corliss, W. Kunnmann, R. Thomas, R. J. Begum, and P. Bak, *Observation of an unusual magnetic phase transition in Nd Sn$_3$*, Phys. Rev. B 22 (1980), pp. 1327-1330.

[11] C. Stassis, J. Zarestky, K. Loong, O. D. McMasters, and R. M. Nicklow, *Lattice dynamics of LaSn$_3$*, Phys. Rev. B 23 (1981), pp. 2227-2234.

[12] K. Ikeda, and A. A. Gschneidner Jr., *Quenching of spin fluctuations by high magnetic fields in the heat capacity of CeSn$_3$*, Phys. Rev. B 25 (1982), pp. 4623-4632.

[13] S. Cirafici, F. Canepa, G. L. Olcese, and G. Costa, *High temperature heat capacity of the LaSn$_3$ and CeSn$_3$ compounds*, Solid State Commun. 44 (1982), pp. 1507-1510.

[14] F. Canepa, G. A. Costa, and G. L. Olcese, *Thermodynamics and magnetic properties of LaPb$_3$ and CePb$_3$* Solid State Commun. 45 (1983), pp. 725-728.

[15] A. P. Murani, *Magnetic spectral response in the intermetallic compound CeSn$_3$*, Phys. Rev. B 28 (1983), pp. 2308-2311.

[16] T.-W. E. Tsang, K. A. Gschneidner, Jr.,, O. D. McMasters, R. J. Stierman, and S. K. Dhar, *Anisotropic spin fluctuations in cubic CeSn$_3$*, Phys. Rev. B 29 (1984), pp. 4185-4188(R).

[17] N. Gambio, P. Rebouillon, J. P. Bros, G. Borzone, G. Cacciamani, and R. Ferro, *Capacites calorifiques molaires des composes definis CePb$_3$, LaPb$_3$ et NdPb$_3$ a haute temperature*, Journal of the less-Common Metals 154 (1989), pp. 195-205 .

[18] I. Umehara, N. Nagai, and Y. Onuki, *High Field Magnetoresistance and de Haas-van Alphen Effect in LaIn$_3$*, J. Phys. Soc. Jpn. 60 (1991), pp. 591-594.

[19] K. J. Kim, *Optical transitions in CeSn$_3$ and LaSn$_3$*, J. Phys.: Condens. Matter 4 (1992), pp. 8039-8044.

[20] A. P. Murani, A. D. Taylor, R. Osborn, and Z. A. Bowden, *Evolution of the spin-orbit excitation with increasing Kondo energy in CeIn$_{3x}$Sn$_x$*, Phys. Rev. B 48 (1993), pp. 10606-10609(R) .

[21] J. Y. Rhee, B. N. Harmon, and D. W. Lynch,*Optical properties and electronic structures of CeSn$_3$ and LaSn$_3$*, Phys. Rev. B 50 (1994), pp. 5693-5694.

[22] Z. Kletowski, R. Fabrowski, P. Slawinski, and Z. Henkie,*Resistance of some REMe$_3$ compounds, RE=La and Lu, Me=Sn, Pb, In, and Ga*, J. Magn. Magn. Mater. 166 (1997), pp. 361-364.

[23] H. Suzuki, H. Kitazawa, T. Naka, J. Tang, and G. Kido, *Studies of pressure effects on the heavy fermion compound of CePb$_3$*, Solid State Commun. 9 (1998), pp. 447-452.

[24] Z. Kletowski, *High field magnetoresistance of some REIn$_3$ compounds, RE=La, Ce, Pr and Sm*, J. Magn. Magn. Mater. 186 (1998), pp. L7-L9.

[25] K. Kanai, Y. Tezuka, T. Terashima, Y. Muro, M. Ishikawa, T. Uozumi, A. Kotani, G. Schmerber, J. P. Kappler, J. C. Parlebas, and S. Shin, *Resonance effect on inverse-photoemission spectroscopy of CeRh$_3$, CePd$_3$, and CeSn$_3$*, Phys. Rev. B 60 (1999), pp. 5244-5250.

[26] R. Küchler, P. Gegenwart, J. Custers, O. Stockert, N. Caroca-Canales, C. Geibel, J. G. Sereni, and F. Steglich, *Quantum Criticality in the Cubic Heavy-Fermion System CeIn$_{3x}$Sn$_x$*, Phys. Rev. Lett. 96, (2006), pp. 256403-1-256403-4.

[27] E M Bittar, C. Adriano, C. Giles, C. Rettori, Z. Fisk and P. G. Pagliuso, *Electron spin resonance study of the LaIn$_{3x}$Sn$_x$ superconducting system*, J. Phys.: Condens. Matter 23 (2011), pp. 455701-1-455701-5.

[28] M. Shimozawa, S. K. Goh, T. Shibauchi, and Y. Matsuda, *From Kondo lattices to Kondo superlattices*, Reports on progress in phyiscs 79 (2016), pp. 074503-1-074503-21.

[29] M. Shafiq, M. Yazdani-Kachoei c , S. Jalali-Asadabadi, and I. Ahmad, *Electric field gradient analysis of RIn$_3$ and RSn$_3$ compounds (R = La, Ce, Pr and Nd)*, Intermetallics 91 (2017), pp. 95-99.

[30] R. Sharma, G. Ahmed, and Y. Sharma, *Intermediate coupled superconductivity in yttrium intermetallics*, Physica C 540 (2017), pp. 1-15.

[31] D. D. Koelling, *The Fermi surface of CeSn$_3$ and LaSn$_3$*, Solid State Commun. 43 (1982), pp. 247-251.

[32] T. Shao-ping, Z. Kai-ming, and X. Xi-de, *The electronic structures of LaSn$_3$, and LaIn$_3$*, J. Phys.: Condens. Matter 1 (1989), pp. 2677-2682.

[33] Swetarekha Ram, V. Kanchana, G. Vaitheeswaran, A. Svane, S. B. Dugdale, and N. E. Christensen, *Electronic topological transition in LaSn$_3$ under pressure*, Phys. Rev. B 85 (2012), pp. 174531-1-174531-8.

[34] J. A. Abraham, G. Pagare, S. S. Chouhan, and S. P. Sanyal, *Structural, electronic, elastic, mechanical and thermal behavior of RESn$_3$ (RE = Y, La and Ce): A first principles study*, Intermetallics 51 (2014), pp. 1-10.

[35] J. A. Abraham, G. Pagare, S. S. Chouhan, and S. P. Sanyal, *High pressure structural, elastic, mechanical and thermal behavior of LaX$_3$ (X = In, Sn, Tl and Pb) compounds: A FP-LAPW study*, Computational Materials Science 81 (2014), pp. 423-432.

[36] X. Luo, D. F. Shao, Q. L. Pei, J. Y. Song, L. Hu, Y. Y. Han, X. B. Zhu, W. H. Song, W. J. Lu, and Y. P. Sun, *Superconductivity in CaSn$_3$ single crystals with a AuCu$_3$-type structure*, J. Mater. Chem. C 3 (2015), pp. 11432-11438.

[37] P. Giannozzi, S. Baroni, N. Bonini, M. Calandra, R. Car, C. Cavazzoni, D. Ceresoli, G. L. Chiarotti, M. Cococcioni, I. Dabo, A. D. Corso, S. de. Gironcoli, S. Fabris, G. Fratesi, R. Gebauer, U. Gerstmann, C. Gougoussis, A. Kokalj, M. Lazzeri, L. Martin-Samos, N. Marzari, F. Mauri, R. Mazzarello, S. Paolini, A. Pasquarello, L. Paulatto, C. Sbraccia, S. Scandolo, G. Sclauzero, A. P. Seitsonen, A. Smogunov, P. Umari, and R. M. Wentzcovitch, *QUANTUM ESPRESSO: a modular and open-source software project for quantum simulations of materials*, J. Phys.: Condens. Matter 21 (2009), pp. 395502-1-395502-19.

[38] P. B. Allen, and R. C. Dynes, *Transition temperature of strong-coupled superconductors reanalyzed*, Phys. Rev. B 12 (1975), pp. 905-922.

[39] J.P. Perdew, A. Ruzsinszky, G.I. Csonka, O.A. Vydrov, G.E. Scuseria, L.A. Constantin, X. Zhou, and K. Burke, *Restoring the Density-Gradient Expansion for Exchange in Solids and Surfaces*, Phys. Rev. Lett. 100 (2008), pp. 136406-1-136406-4.

[40] D. Vanderbilt,*Soft self-consistent pseudopotentials in a generalized eigenvalue formalism*, Phys. Rev. B 41 (1990), pp. 7892-7895 (R).

[41] A. M. Rappe, K. M. Rabe, E. Kaxiras, and J. D. Joannopoulos,*Optimized pseudopotentials*, Phys. Rev. B 41 (1990), pp. 1227-1230 (R).

[42] W. Kohn, and L. J. Sham, *Self-Consistent Equations Including Exchange and Correlation Effects*, Phys. Rev. 140 (1965), pp. A1133-A1138.

[43] H. J. Monkhorst, and J. D. Pack, *Special points for Brillouin-zone integrations*, Phys. Rev. B 13 (1976), pp. 5188-5192.

[44] S. B. D. Dugdale, *First-principles study of electron-phonon superconductivity in YSn$_3$*, Phys. Rev. 82 (2011), pp. 012502-1-012502-4.

[45] A. B. Migdal,*Interaction between electrons and lattice vibrations in a normal metal*, Zh. Eksp. Teor. Fiz. 34 (1958), pp. 996-1001.

[46] G. M. Eliashberg,*Interaction between electrons and lattice vibrations in a superconductor*, Sov. Phys. JETP. 11 (1960), pp. 696-702.

[47] H. M. Tütüncü, H. Y. Uzunok, Ertuğrul Karaca, G. P. Srivastava, S. Özer, and Ş. Uğur,*Ab initio investigation of BCS-type superconductivity in LuNi$_2$B$_2$C-type superconductors*, Phys. Rev. B 92 (2015), pp. 054510-1-054510-17.

[48] Feliciano Giustino, Marvin L. Cohen, and Steven G. Louie, *Electron-phonon interaction using Wannier functions*, Phys. Rev. B 76 (2007) 165108-1-165108-19.

[49] D. Raczkowski, A. Canning, and L. W. Wang, *Thomas-Fermi charge mixing for obtaining self-consistency in density functional calculations*, Phys. Rev. B 64 (2001) 121101(R)-1-121101(R)-4.

[50] H. Fröhlich, *Theory of the Superconducting State. I. The Ground State at the Absolute Zero of Temperature*, Phys. Rev. 79 (1950) 845-856.

[51] F. D. Murnaghan,*The Compressibility of Media under Extreme Pressures*, Proc. Nat. Acad. Sci. 30 (1944), pp. 244-247.

Table 1. The calculated values of lattice constant (a), volume (V), nearest neighbour distance (d), bulk modulus (B) and its pressure derivative ($B^{'}$) for LaSn$_3$ and CaSn$_3$ and their comparison with previous experimental and theoretical results.

Source	$a(\AA)$	$V(\AA^3)$	d ($\AA$)	B(GPa)	$B^{'}$
LaSn$_3$	4.739	106.43	3.351	62.3	4.68
Experimental [3]	4.771	108.60			
Experimental [11]				55.1	
LMTO-ASA [32]	4.73	105.82	3.345	78.0	
GGA [33]	4.81	111.28	3.401	55.5	
LDA [33]	4.70	103.82	3.323	68.2	
GGA [34, 35]	4.780	109.22	3.379	57.5	4.98
CaSn$_3$	4.694	103.43	3.319	50.3	4.39
Experimental [36]	4.742	106.63			

Table 2.　The calculated values of physical quantities related to superconductivity in LaSn$_3$ and CaSn$_3$ with the use of theoretical and experimental values of lattice parameter.

| Compound	N(E$_F$) (States/eV)	ω_{ln} (K)	λ	T$_c$ (K)
LaSn$_3$ ($a_{theoretical}$)	2.582	105.63	0.876	5.90
LaSn$_3$ ($a_{experimental}$)	2.606	100.39	0.937	6.30
GGA [34, 35]	3.060			
LMTO-ASA [32]	2.150			
LDA [33]	2.670		0.86	8.10
Experimental [1]				6.45
Experimental [5]	2.600		0.80	
Experimental [6]				6.45
Experimental [9]	2.800			
Experimental [27]				6.40
CaSn$_3$ ($a_{theoretical}$)	1.215	108.85	0.642	3.03
CaSn$_3$ ($a_{experimental}$)	1.216	100.31	0.725	3.80
Experimental [36]			0.650	4.20
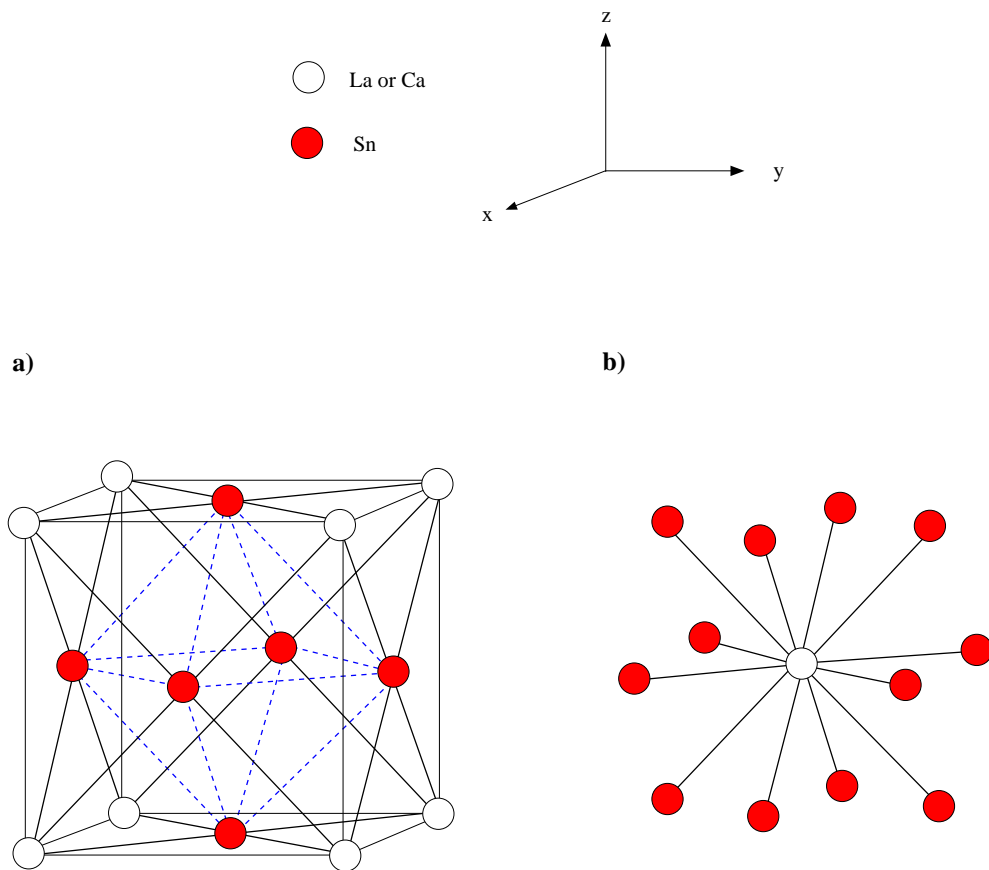
Figure 1. (a) The AuCu$_3$ crystal structure of LaSn$_3$ and CaSn$_3$. Each Sn atom is surrounded by four La (or Ca) atoms. (b) Each La (or Ca) atom is surrounded by twelve Sn atoms.
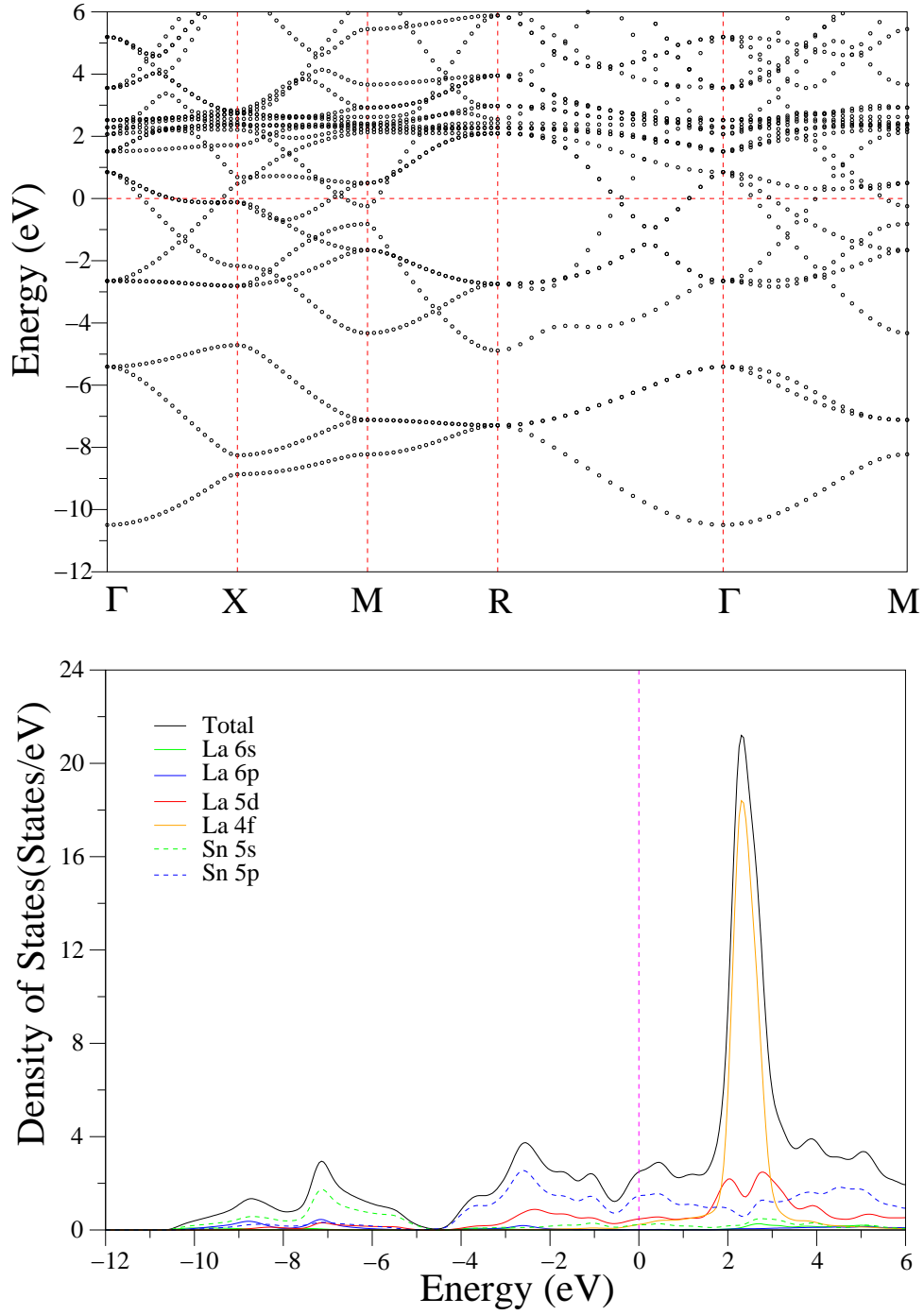
Figure 2. The electronic band structure and electronic density of states for the simple cubic LaSn$_3$. The Fermi energy is set to 0 eV.
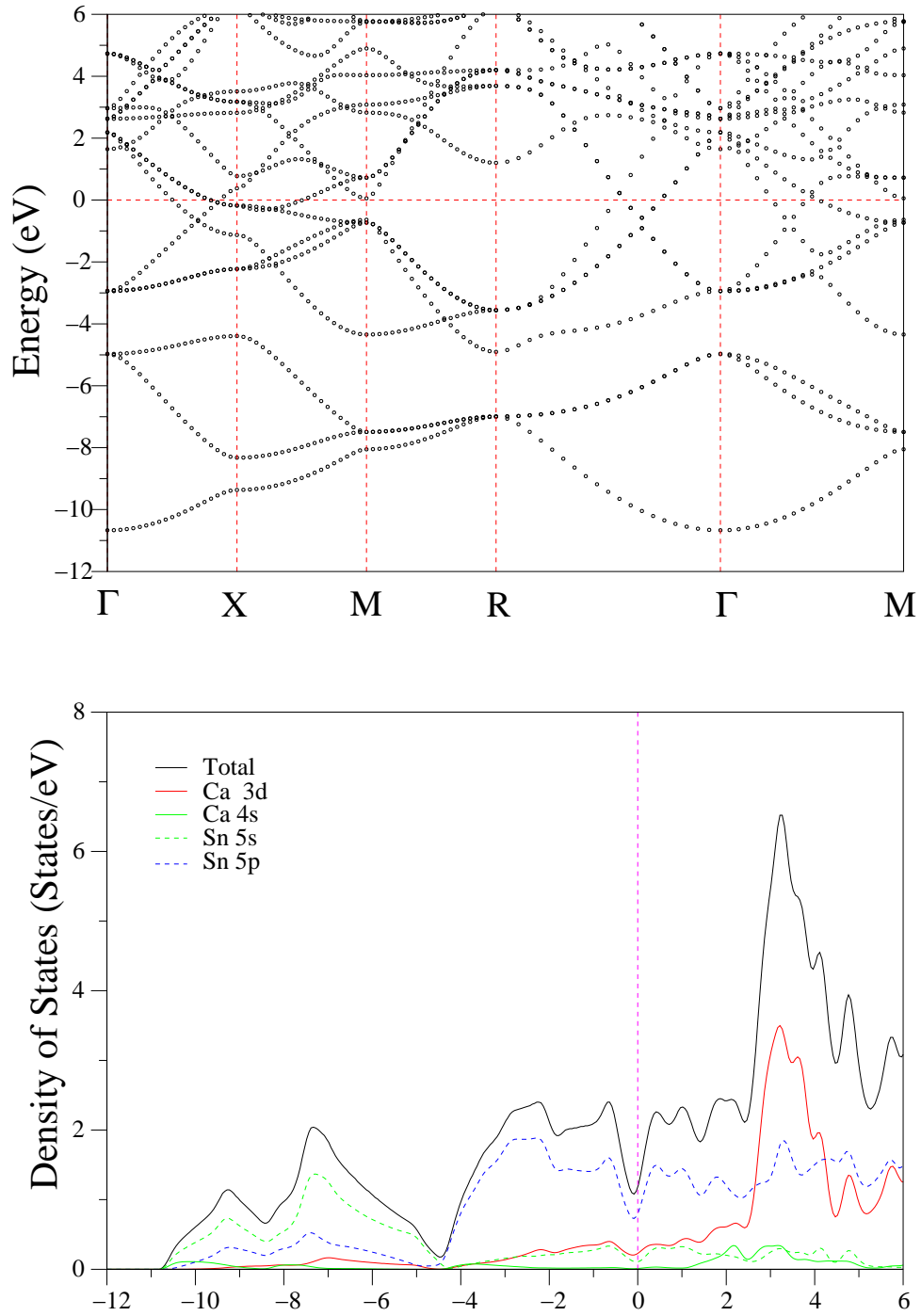
Figure 3. The electronic band structure and electronic density of states for the simple cubic CaSn₃. The Fermi energy is set to 0 eV.
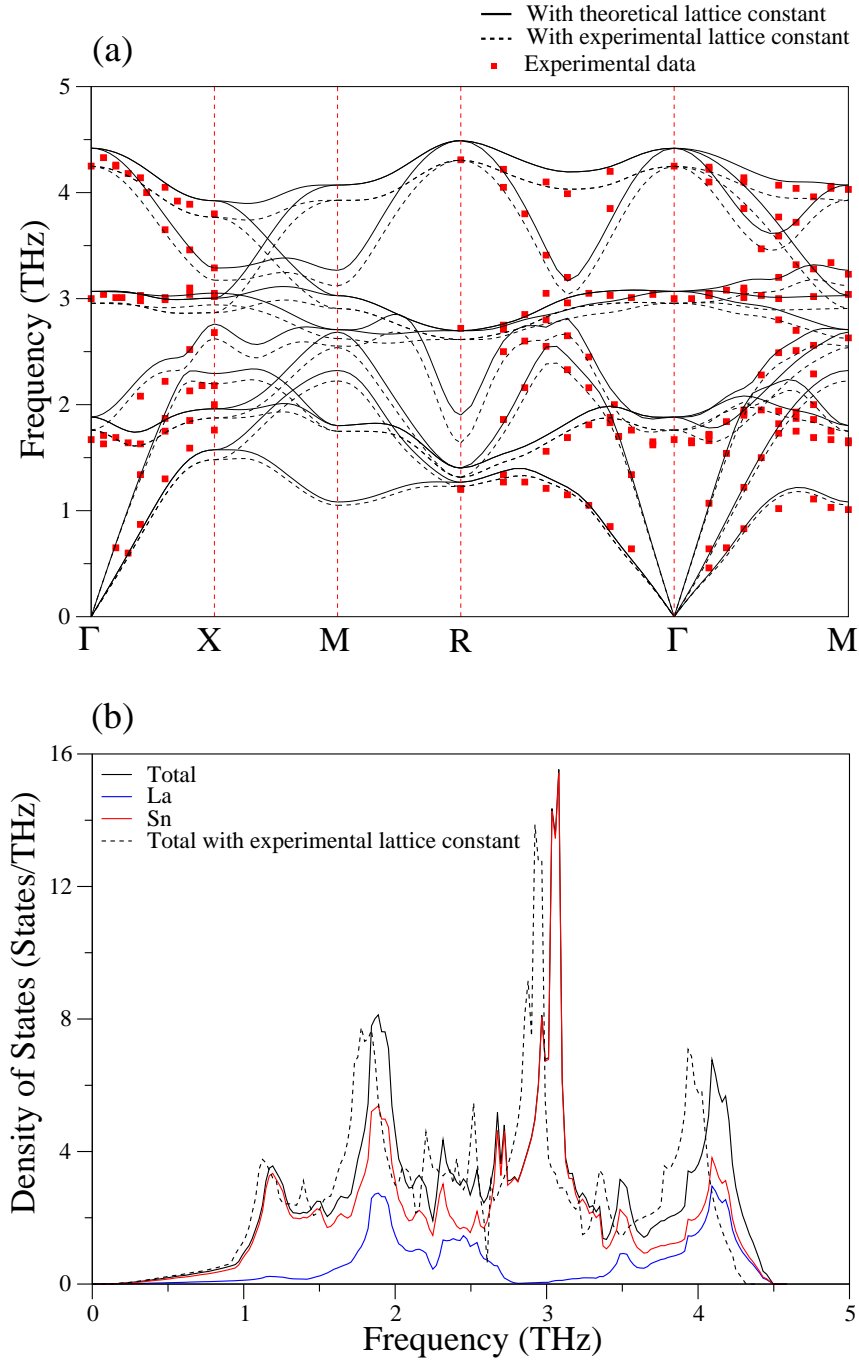
H. Y. Uzunok, H. M. Tütüncü, Ertuğrul Karaca, A. Başoğlu, G. P. Srivastava

Figure 4. (a) The phonon dispersion curves for LaSn$_3$ along selected symmetry directions in the simple cubic Brillouin zone. The solid lines and dashed lines display the calculated phonon branches with the use of theoretical and experimental values of lattice parameter, respectively. Inelastic neutron scattering results [11] are shown by filled red squares. (b) The total and partial phonon density of states for LaSn$_3$. The dashed line displays total DOS obtained using the experimental value of lattice parameter.
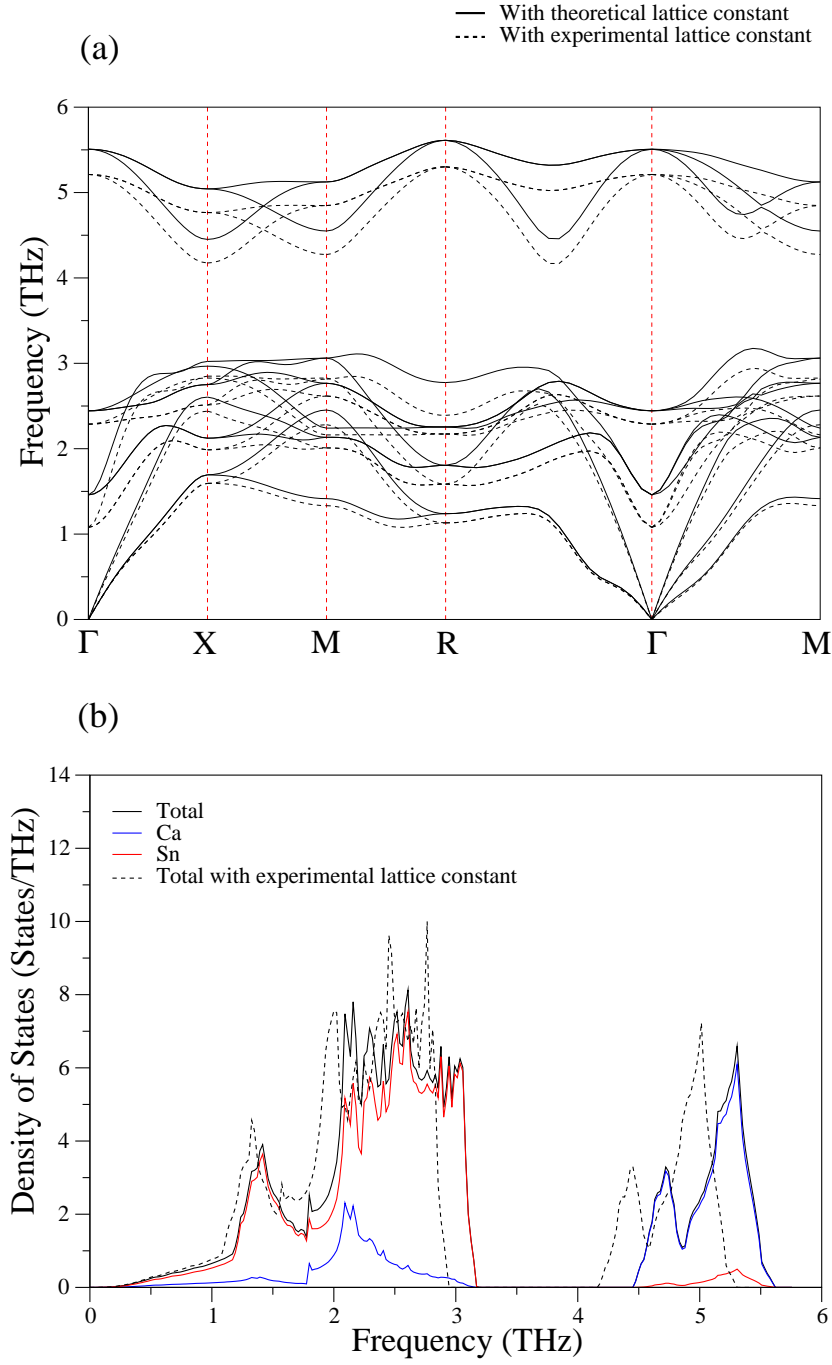
(a)

(b)

Figure 5. (a) The phonon dispersion curves for CaSn$_3$ along selected symmetry directions in the simple cubic Brillouin zone. The solid lines and dashed lines display the calculated phonon branches with the use of theoretical and experimental values of lattice parameter. (b) The total and partial phonon density of states for CaSn$_3$. The dashed line displays total DOS obtained using the experimental value of lattice parameter.
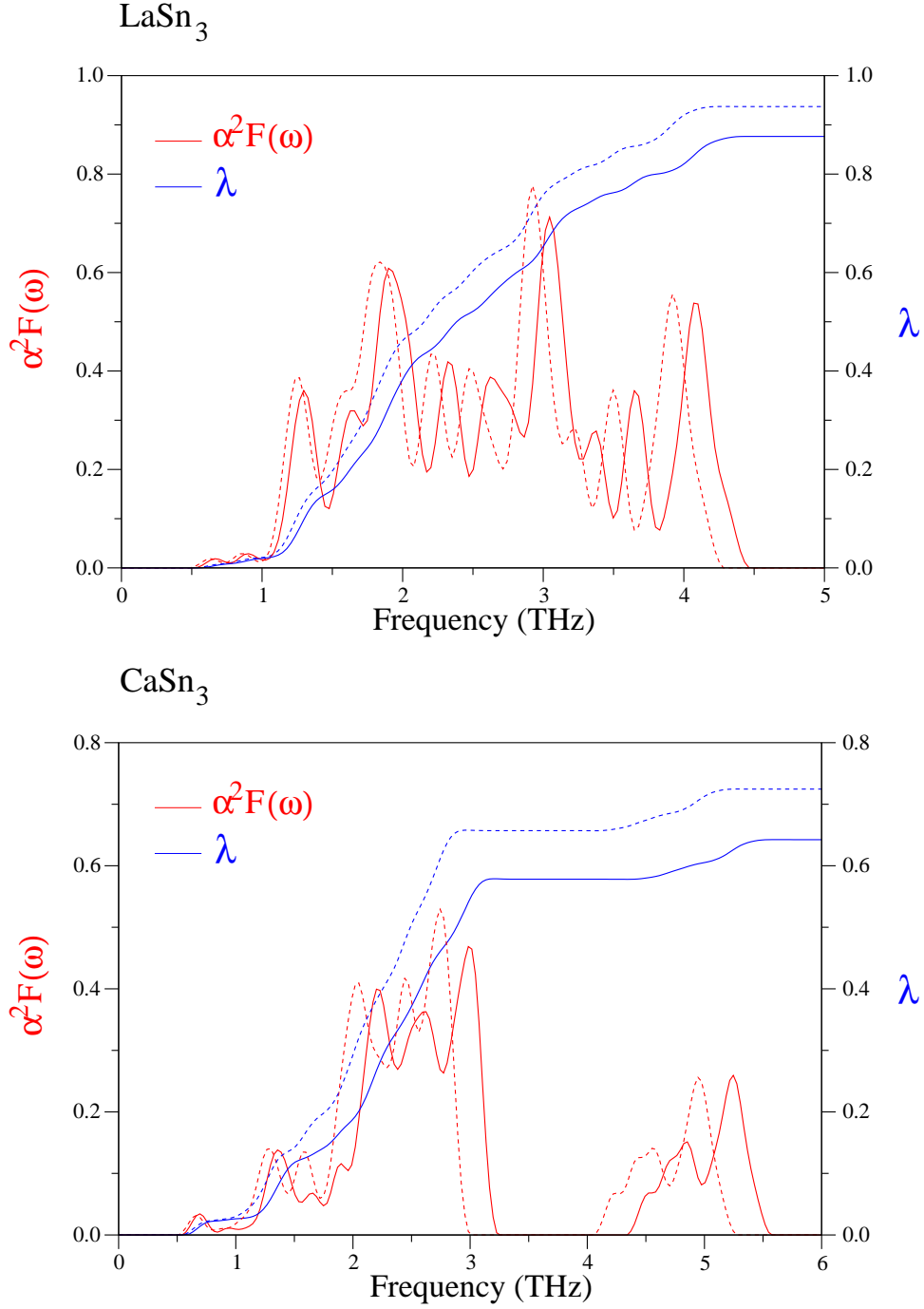
H. Y. Uzunok, H. M. Tütüncü, Ertuğrul Karaca, A. Başoğlu, G. P. Srivastava

Figure 6. Eliashberg spectral function $\alpha^2 F(\omega)$ (red line) and integrated electron-phonon coupling parameter λ (blue line) for LaSn$_3$ and CaSn$_3$. The corresponding results with the use of experimental lattice constant are illustrated by dashed lines.